J Mater Sci (2008) 43:3697–3703
DOI 10.1007/s10853-008-2593-2

Dynamic mechanical thermal analysis of all-PP composites based on β and α polymorphic forms

Thomas N. Abraham · S. Siengchin · J. Karger-Kocsis

Received: 14 January 2008 / Accepted: 12 March 2008 / Published online: 4 April 2008

Abstract All polypropylene (all-PP) composites were manufactured by exploiting the polymorphic forms of PP, in which alpha (α)-PP tapes worked as reinforcement and beta (β)-PP served as matrix. The mechanical performance of the composite was investigated in a range of frequencies and temperatures using dynamic mechanical thermal analysis (DMTA). The volume fractions of matrix and reinforcement were estimated using optical microscope images. Both the DMTA and the static flexural bending tests revealed that the α-PP tapes act as an effective reinforcement for the β-PP matrix. Time–temperature superposition (TTS) was applied to estimate the stiffness of the composites as a function of frequency ($f = 10^{-9}...10^{23}$) in the form of a master curve. The Williams–Landel–Ferry (WLF) model described properly change in the experimental shift factors used to create the storage modulus versus frequency master curve. The activation energies for the α and β relaxations were also calculated by using the Arrhenius equation.

Introduction

Single thermoplastic composites (also termed thermoplastic homocomposites) have drawn research interest in recent years because of their environment-friendly character. All polypropylene (all-PP) is a single thermoplastic polymer composite which represents an effective alternative to the traditional fibre reinforced composites. Here the matrix and the reinforcement are from the same polymer, thereby supporting the ease of recyclability. Several techniques have been reported for the production of single thermoplastic polymer composite materials, such as film stacking followed by melting [1, 2], hot compaction [3], powder and solution impregnation [4]. The basic principle behind all these techniques is to exploit the melt temperature difference between the oriented or highly stretched material (which should act as the reinforcement) and the same material without orientation (taking over the role of the matrix). Besides recyclability, the interest for single polymer composites is based upon the expectation that a good interfacial bonding can be achieved if matrix and reinforcement are made from the same semicrystalline polymer [5, 6].

One of the promising approaches in the development of all-PP composites is to exploit the polymorphism-related difference in the melting range between the beta(β)-(matrix) and alpha(α)-phases (reinforcement) PPs [2, 7]. An all-PP composite has been made in our laboratory with α-PP tapes as the reinforcement and β-PP film as the matrix. However, the entirely thermoplastic nature of these composites raises important questions regarding the viscoelastic behaviour at elevated temperatures. To provide information about the viscoelastic properties, various experimental techniques can be used, among which the dynamic mechanical thermal analysis (DMTA) offers adaptable test procedures. Long-term viscoelastic properties of all-PP composite laminate have been investigated by using the time–temperature superposition principle [8, 9]. Nevertheless, it is understood that these properties significantly govern the applicability of the material. The main aim of this paper is to investigate the response of a novel all-PP composite to mechanical loading in a broad range of

T. N. Abraham · S. Siengchin · J. Karger-Kocsis (✉)
Institut für Verbundwerkstoffe GmbH, (Institute for Composite Materials), University of Kaiserslautern, 67663 Kaiserslautern, Germany
e-mail: karger@ivw.uni-kl.de

temperature and frequencies. By using the DMTA responses, master curves can be created to predict the performance of all-PP composites at much lower and higher frequencies than achievable in the laboratory.

Materials

Manufacture of laminates

The PP tapes used for the manufacture of laminates were produced in our laboratory using a twin-screw extruder. The temperature zones in the extruder were maintained at 190, 200, 210 and 220 °C from the feeder to the nozzle. The die used had a dimension of 10 × 2 mm^2. The characteristics of PP tapes used for the preparation of the laminates are summarized in Table 1. A thin film of beta polymorph rich isotactic PP (β-PP) served as the matrix. The thin film (120 μm thickness) was obtained by compression moulding β-nucleated PP sheet of Tipplen H 483 F (melt flow index 6.5 g/10 min at 230 °C and 2.16 kg load) at 180 °C for 5 min. The manufacture of the PP laminates involved a two-stage process: winding of the PP tapes in a cross-ply manner (0/90°;CP), and consolidation of the related tape consisting fabric using hot compaction. The schematic of the tape winding process is shown in Fig. 1. Before winding the PP tapes a thin β-PP film layer was placed on the surface of a thin steel plate. Using a typical winding machine, supplied by Bolenz & Schaefer Maschinenfabrik (Biedenkopf, Germany), PP tapes were wound from a bobbin onto the same steel plate rotating at a constant speed. After laying one layer of PP tape another layer of β-PP film was placed and the winding direction on the steel plate was changed. The same process continued and the total number of layers of PP tapes and β-PP film was kept as four and five, respectively. A similar winding process was already adopted for manufacturing CP type all-PP composite from coextruded Pure® tapes [10, 11].

All-PP composite laminates were produced by the well-known hot compaction method in a hot press (P/O/Weber GmbH, Remshalden, Germany) at a temperature of 160 °C and a holding time of 5 min under high pressure (7 MPa).

Table 1 Summary of PP tape

Width	1.5 mm
Thickness	265 μm
Density	901 ± 9 kg/m^3
Composition	Homopolymer (Novolen 1104 H melt flow index 2 g/10 min at 230 °C and 2.16 kg load)
Tensile modulus (ISO 527)	4 ± 0.5 GPa

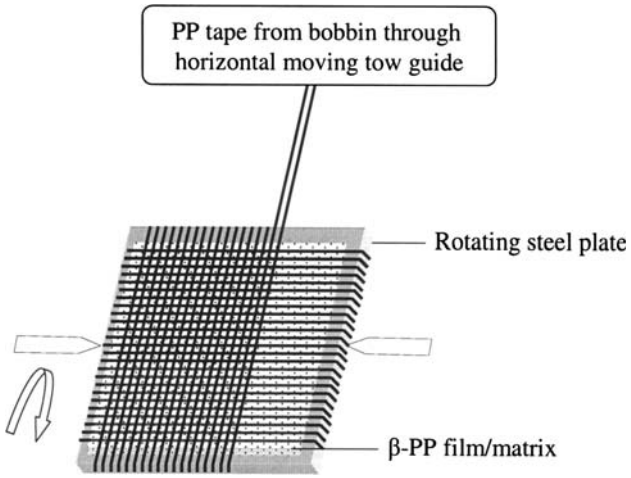

Fig. 1 Scheme of the tape winding process for the fabrication of all-PP composites

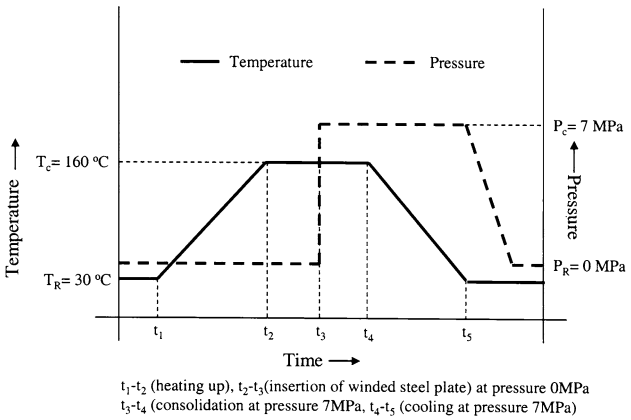

Fig. 2 Schematic of time–temperature and time–pressure profile used for consolidation of all-PP by hot compaction (T_R and T_C are release and consolidation temperatures, respectively; P_R and P_C are release and consolidation pressures respectively)

The time–temperature profile during the consolidation is shown schematically in Fig. 2.

Experimental procedures

Differential scanning calorimetry (DSC)

The presence of β-PP and the occurrence of β–α transformation were demonstrated by DSC using a Mettler-Toledo DSC821 instrument (Greifensee, Switzerland). In order to demonstrate the difference between the α and β modifications, the first heating scan ($T = 25$ to 200 °C) was followed by a cooling one to $T = 100$ °C, prior to a second heating cycle to $T = 200$ °C. This heating cooling programme was selected based on the recommendation of Varga et al. [12].

Optical microscopy

Microscopic images of the cross-section of the all-PP laminates were captured by a stereomicroscope (Leitz, Germany) equipped with a high-resolution digital camera. The IMAGE-C analysis software was used to estimate the void content from the micrographs.

DMTA of all-PP composites

DMTA of all-PP composite laminates was performed in dual cantilever flexural mode. Specimen were cut from the composite plates with dimensions of approximately 60 mm × 15 mm × 2 mm (length × width × thickness) in the DMTA Q800 (TA Instruments, New Castle, USA) machine equipped with a data acquisition software. The specimens were cooled to −50 °C. The temperature was allowed to stabilize and then increased by 3 °C, kept 5 min isothermal, until 120 °C. The specimen was subjected to a sinusoidal flexural displacement applying a maximum tensile strain of 0.1% (which was well within the viscoelastic region) at frequencies 0.01, 0.1, 1, 5 and 10 Hz at all isothermal temperatures. For each frequency, the complex dynamic modulus (E') and loss factor ($\tan\delta$) were recorded.

Theoretical background

An attempt was made to apply the time–temperature superposition (TTS) to the DMTA data measured as function of both temperature ($T = -50$ °C...+120 °C) and frequency ($f = 0.01...10$ Hz) using rheology advantage data analysis software provided by TA Instruments. Master curves in the form of storage modulus (E') versus frequency were produced by superimposing the storage modulus versus frequency traces using the TTS principle. A reference temperature (T_{ref} = 22 °C) was used for this superposition (shifting) process. The related shift factor a_T is given by Eq. 1:

$$a_T = \frac{E'(T)}{E'(T_{ref})} \tag{1}$$

The shift factors of a master curve have some relationship with temperature. Fitting the experimentally determined shift factors to a mathematical model permits the creation of a master curve in the form of storage modulus versus frequency. With a multi-frequency measurement, frequencies beyond the measurable range of the DMTA can be achieved by using the superposition method based on the Williams–Landel–Ferry (WLF) equation [13, 14]. For the temperature range above the glass-transition temperature, it is generally accepted that the shift factor–temperature relationship is best described by WLF equation:

$$\log a_T = \log\left(\frac{f}{f_0}\right) = \frac{-C_1(T - T_{ref})}{C_2(T - T_{ref})} \tag{2}$$

where C_1 and C_2 are constants.

From the temperature dependence of the shift factor, the activation energy (E_a) can be computed by the following Eq. 3:

$$\ln a_T = \frac{E_a}{R}\left(\frac{1}{T} - \frac{1}{T_{ref}}\right) \tag{3}$$

Static flexural test

The static flexural properties of the all-PP composites, such as modulus of elasticity and ultimate flexural strength, were determined following the DIN EN ISO 178 standard on a Zwick 1445 test machine. Specimens of the same dimensions used for the DMTA test were employed for the three-point bending measurement. A support span of 32.8 mm was used in the three-point bending setup. The cross-head speed of 1 mm/min was applied during the test and the elastic modulus was calculated in the strain range of 0.05–0.25%. Load was applied using a U2 A type 10-kN load cell. A preload of 5 N was applied in the beginning of each test and the mean value of five specimens tested was reported.

Results and discussion

DSC traces of all-PP composite and β-PP film are represented in Fig. 3. The melting temperature of the β modification of isotactic PP ($T_m \approx 154$ °C) homopolymer is lower than that of the reinforcing α-PP tape ($T_m \approx 165$ °C). The DSC trace of the all-PP composite also shows another interesting phenomenon of transformation of β-PP to α form at temperatures above the melting point of the former. This phenomenon has already been observed by Padden and Keith [15]. Samuels and Yee [16], who have conducted extensive studies on the unit cell of β-polypropylene, have concluded that the transformation from the β to the α form must occur through a melt recrystallization process, since the two unit cells are very different.

A typical dynamic mechanical behaviour of the PP tapes, β-PP matrix and all-PP composite laminates at 1 Hz frequency is represented in Fig. 4. It shows that at subambient temperature (the glassy region of PP) the stiffness of PP tape is found to be fairly high. With increasing temperature the E' decreases, as expected. Above 25 °C the stiffness of the tapes drops significantly. Although the tapes lost much of their elastic response above this temperature, their residual stiffness at 120 °C (end of the test) is still higher ($E' = 1$ GPa) than that of an isotropic PP. The high stiffness is attributed to the highly oriented crystals and polymer

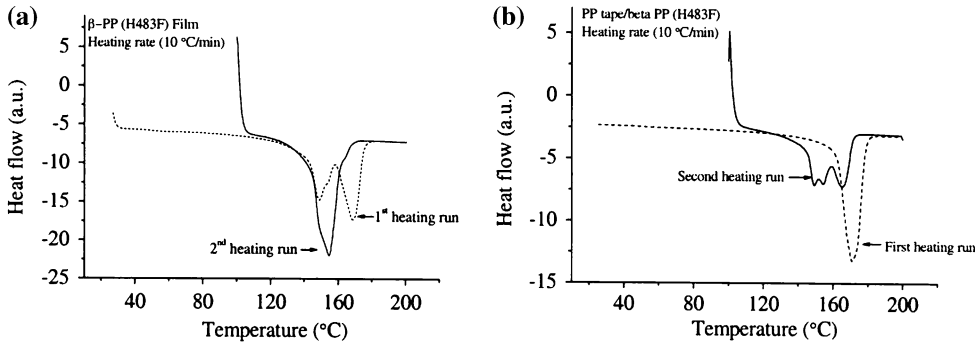

Fig. 3 DSC traces of (**a**) β-PP matrix and (**b**) all-PP composite laminates (β-PP was cooled to $T = 100$ °C prior to its second heating)

chains in the stretching direction of the tape. This implies that the tape possesses a residual orientation even at this higher temperature. The results also indicate that the stiffness of all-PP composite laminate is higher than that of the matrix (β-PP), and confirm the reinforcement effect of α-PP tapes on β-PP matrix. At room temperature the E' of PP tape, all-PP composite laminate and β-PP matrix are 4.8, 2.9 and 2.2 GPa respectively.

Figure 4 also exhibits the course of tanδ (ratio of E''/E') with temperature, which shows a maximum at $\approx$80 °C. The maximum tanδ value recorded for the all-PP tape was 0.15. The tanδ peaks represent different relaxation transitions [12]. However, in Fig. 3 PP tape does not resolve any tanδ peak corresponding to the glass transition of PP ($T_g \approx -10$ °C–0 °C), but a more definite tanδ peak is seen corresponding to the α transition (T_α) at approximately 80 °C. Since these tapes are produced by stretching, the amorphous phase becomes highly oriented between the crystalline regions and it has less freedom to be involved in segmental motions [17]. Therefore, in highly oriented PP systems, the magnitude of T_g peaks is greatly reduced compared to isotropic PP. While T_g reflects mobility within the amorphous regions, T_α dictates the onset of segmental motion within the crystalline regions [13, 18, 19]. The loss

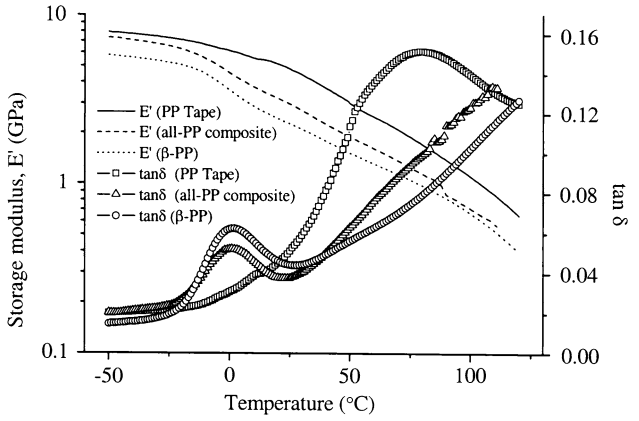

Fig. 4 DMA plots of storage modulus and tanδ versus temperature for α-PP tape, all-PP composite laminates and β-PP matrix at frequency 1 Hz (note: log scale of E')

factor as a function of temperature for all-PP composite and β-PP matrix is also shown in Fig. 4. The result shows a clear tanδ peak corresponding to β relaxation (T_g) near 0 °C for both the β-PP matrix and all-PP composite. The position of T_g remained nearly unchanged, but the peak intensity and magnitude decreased significantly which indicates the increase in stiffness as result of reinforcement of the β-PP matrix.

It has been shown that a simple rule of mixtures can be very useful in helping to understand the in-plane properties of compacted single polymer composites. A model based on a parallel rule of mixtures and knowledge of the properties of the oriented and matrix phases and fraction of the two phases have been reported by Hine et al. [20]. The compacted sheet modulus ($E_{\text{compacted sheet}}$) can then be shown simply to be given by Eq. 4

$$E_{\text{compacted sheet}} = E_{\text{tape}} \frac{V_{\text{tape}}}{2} + E_{\text{matrix/film}} \left(\frac{1 + V_{\text{matrix/film}}}{2} \right) \quad (4)$$

where E_{tape} and $E_{\text{matrix/film}}$ are the modulus of the oriented and matrix phases, respectively (assuming same chemical composition for both the matrix and reinforcement, i.e. PP), and V is the appropriate fraction of each component. The volume fraction of each component is obtained from the optical micrographs shown in Fig. 5. Using the IMAGE-C analysis software, the volume fraction of the reinforcing tapes was determined and found to be 50%. The storage modulus values obtained from DMTA for the PP tape and the β-PP matrix at the same strain rate at room temperature were applied in equation for predicting the in-plane modulus of the compacted sheet. The predicted modulus (3 GPa) is comparable with the experimental measurements (2.9 GPa), and indicates that this simple approach predicts the modulus quite satisfactorily.

Storage modulus for a wider range of frequencies can be obtained by TTS using the data from multi-frequency DMTA tests. Figure 6 shows the variation of storage modulus for a range of temperatures between −20 and 80 °C for the all-PP composites tested at 0.01, 0.1, 1, 5 and 10 Hz, respectively. An increase in the storage modulus for

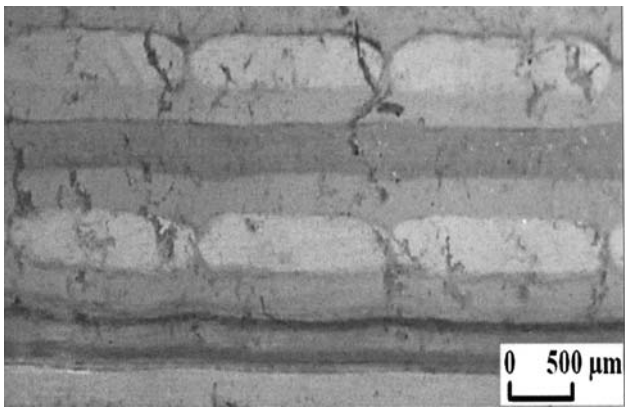

Fig. 5 Optical micrograph from the cross-sections of all-PP composite laminates

all-PP composite laminates with increasing frequency and decreasing temperature is seen, as expected. The variation of tanδ at different frequencies for the all-PP laminates are shown in Table 2. A remarkable influence of frequency was observed for both the α and β relaxations of the composites. The frequency increase shifted the position of the relaxation region to higher temperatures. The tanδ peaks corresponding to the β and α transitions of all-PP composite laminate were found to be at 4 and 97 °C, respectively, at 1 Hz frequency. The T_α peak became broader and less pronounced due to the additional melting region at higher temperatures. Master curves of the storage modulus against frequencies created at a reference temperature of 22 °C are shown in Fig. 7 for the β-PP matrix and the all-PP composite laminates. From the master curve data, the curve approaches a similar plateau value at high frequency, but the terminal region at lower frequencies is more dependent on the reinforcement effect of the composite compared with the β-PP matrix, as expected. The storage modulus master curve provides a useful prediction

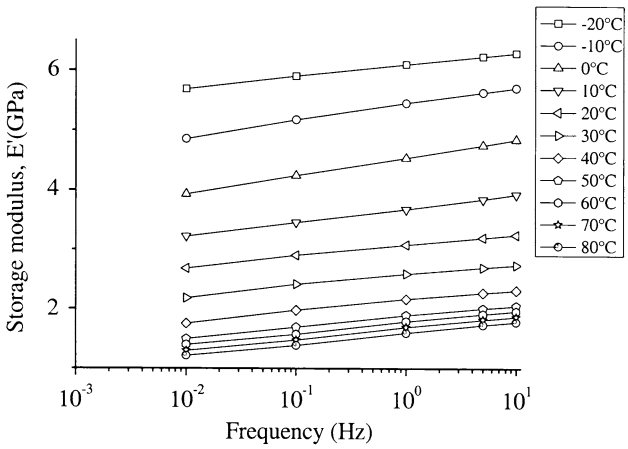

Fig. 6 Storage modulus versus frequency for a range of temperatures for the all-PP composite

Table 2 T_g and T_α at different oscillating frequenies

	T_g (°C)	T_α (°C)
0.01 Hz	0.99	55
0.1 Hz	2.13	81
1 Hz	3.89	97
10 Hz	6.90	–

of the modulus over loading frequencies from 10^{-9} to 10^{23} Hz. However, it must be emphasized that these master curves are quite reliable for short term, but significant deviation may occur at large time scales. Shift factor, a_T was obtained directly from the experimental storage modulus curves against time by measuring the amount of shift along the time scale necessary to superimpose the curves on the reference. The shift factors used for the generation of storage modulus master curve is shown in Fig. 8. We tried the classical WLF equation to describe the relationship between a_T and temperature. It was found that the WLF equation is suitable to describe the temperature dependence.

In Fig. 9, (log a_T) is plotted against the reciprocal of the absolute temperature and the activation energy, E_a, was determined using Eq. 5

$$E_a = m(2.303 \cdot R) \tag{5}$$

where m is the gradient of fit line in (Fig. 9) and R is the universal gas constant (8.314 JK^{-1} mol^{-1}). An activation energy of 346 $kJmol^{-1}$ is obtained, which is of the same order as previously reported to shift the dynamic modulus master curve, using the same Arrhenius shifting of PP [21, 22]. It is likely that this 'activation energy' describes a

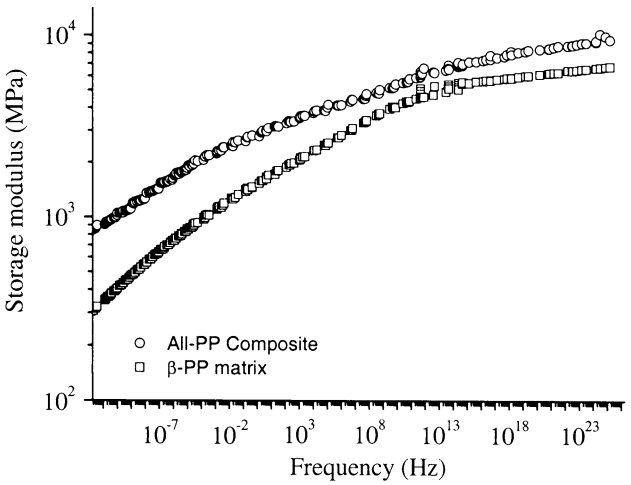

Fig. 7 Storage modulus versus frequency master curves at a reference temperature of 22 °C for β-PP matrix and all-PP composite (note: log scale of y-axis)

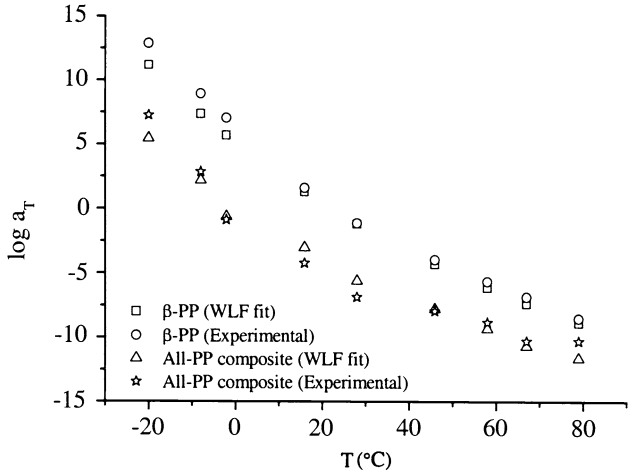

Fig. 8 Experimentally determined shift factors and the WLF fits

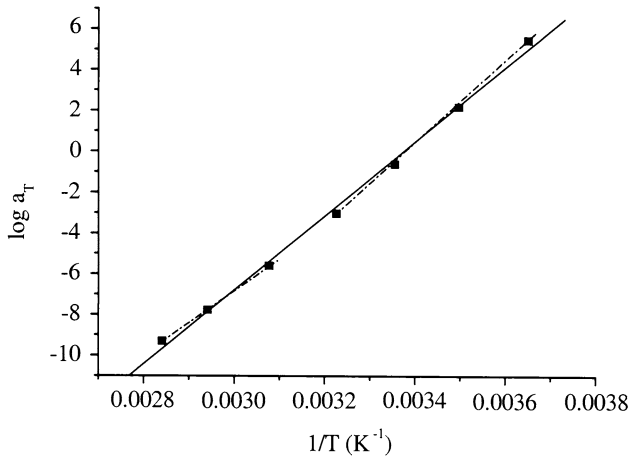

Fig. 9 Dependence of logarithm of shift factor on reciprocal of temperature for all-PP composite; (—) first-order regression line considering one component model; (...) first-order regression line considering two component model

complex combination of effects since the simple time–temperature superposition is only directly applicable to amorphous polymers. A closer view of Fig. 9 reveals that the data points are better fitted by two-component model. A two-component model is significant and offers good insight into the nature of changes of viscoelastic properties of semicrystalline polymers with temperature increase. It can be seen that above 40 °C, the slope of regression curve changes. It is known that PP can undergo a crystalline-phase-related relaxation due to inter-or intra-crystalline motion resulting in a broad relaxation ranging from 40 to more than 100 °C. This is mainly due to the fact that the isotactic PP has a complex morphology. Thus it can undergo different transitions depending on the material and methodology. Using a two-component fit, the activation energies are calculated for the two types of relaxation processes and presented in Table 3. These two activation energies correspond to the α- and β-relaxation processes and are obtained as 155 and 430 kJ mol^{-1} respectively. The activation energy for the β-relaxation process was found to be higher than α-relaxation process, similar to those reported by Dutta and Edward [23].

Table 4 Flexural properties of all-PP composite laminates

Material	Flexural properties		
	Modulus (GPa)	Strength (MPa)	Strain at max. load
β-PP film	1.2 ± 0.17	44 ± 5	5.6 ± 0.2
All-PP composite	2.3 ± 0.07	60 ± 0.5	4.9 ± 0.3

Parallel to the dynamic flexural tests, short-term static flexural tests were also conducted. Table 4 shows a plot of the experimental results obtained from the flexural test of the all-PP composites. The result shows the average value of elastic modulus and maximum flexural strength of the β-PP matrix and the all-PP composite laminates. The stiffness of the all-PP woven composites is to a great extent governed by the stiffness of the tapes in the longitudinal direction [24]. It shows that strength (36%) and stiffness (85%) of the β-PP matrix is improved significantly by reinforcing PP tapes. A detailed study on the flexural behaviour of the all-PP composite (Pure®) was conducted in our laboratory and reported that the short-term as well as long-term viscoelastic behaviours are greatly influenced by the composite morphology, particularly the reinforcement architecture [11].

Conclusion

All-PP composites were produced from α-PP tapes and β-PP film/matrix by a hot consolidation method. This study has proved that extruded α-PP tapes (high melt temperature) can be used for reinforcing the β-PP matrix (low melt

Table 3 Activation energy values calculated for all-PP composite laminates

Material	One-component model	Two-component model	
	Activation energy (kJ/mol)	Activation energy (kJ/mol)	
		α-Relaxation	β-Relaxation
All-PP composite	297	154	430

temperature). At room temperature the E' of the β-PP matrix is increased by 0.7 GPa by the effective reinforcement of α-PP tape obtained by DMTA. Similarly there is an increase in the flexural strength and stiffness of the all-PP composite is also observed. The tanδ peak was not discernable for the reinforcing α-PP tape, while it is clearly identified for the β-PP matrix and the all-PP composite laminate. Though, the position of T_g remained nearly unchanged, the peak intensity and magnitude decreased significantly. The storage modulus master curve approach a similar plateau value at high frequency, but the terminal region at lower frequencies is more dependent on reinforcement effect of composite compared with the β-PP matrix. The experimental shift factors showed a good agreement with both WLF and Arrhenius models. Using a two-component fit, the activation energies are calculated for the α- and β-relaxation processes with the help of Arrhenius equation. The activation energy for the β-relaxation process was found to be higher than α-relaxation process.

Acknowledgement The authors thank the German Science Foundation for the financial support of this project (DFG Ka 1202/17).

References

1. Houshyar S, Shanks RA, Hodzic A (2005) Macromol Mater Eng 290:45. doi:10.1002/mame.200400158
2. Bárány T, Karger-Kocsis J, Czigány T (2006) Polym Adv Technol 17:818. doi:10.1002/pat.813
3. Hine PJ, Ward IM, Jordan ND, Olley R, Bassett DC (2001) J Macromol Sci Phys 40B:959
4. Amornsakchal T, Bassett DC, Olley RH, Hine PJ, Ward IM (2000) J Appl Polym Sci 78:787. doi:10.1002/1097-4628(20001024)78:4≤787::AID-APP110≥3.0.CO;2-A
5. Capiati NJ, Porter RS (1975) J Mater Sci 10:1671. doi:10.1007/BF00554928
6. Mead WT, Porter RS (1978) J Appl Polym Sci 22:3249. doi:10.1002/app.1978.070221119
7. Karger-Kocsis J (2007) Patentschrift DE 10237803B4, Institut für Verbundwerkstoffe GmbH
8. Boiko YuM, Kovriga VV (1993) Intern J Polym Mater 22:209. doi:10.1080/00914039308012076
9. Wortmann FJ, Schulz KV (1995) Polymer 36:315. doi:10.1016/0032-3861(95)91319-3
10. Abraham T, Banik K, Karger-Kocsis J (2007) eXPRESS Polym Lett 1:519. doi:10.3144/expresspolymlett.2007.74
11. Banik K, Abraham T, Karger-Kocsis J (2007) Macromol Mater Eng 292:1280. doi:10.1002/mame.200700180
12. Varga J (2002) J Macromol Sci Part B-Phys 41:1121. doi:10.1081/MB-120013089
13. Williams ML, Landel RF, Ferry JD (1955) J Am Chem Soc 77:3701. doi:10.1021/ja01619a008
14. Ferry JD (1970) Viscoelastic properties of polymers, 2nd edn, Wiley, New York, 292
15. Padden FJ, Keith HD (1959) J Appl Phys 30:1479. doi:10.1063/1.1734985
16. Samuels RJ, Yee RY (1972) J Polym Phys Ed 10:385. doi:10.1002/pol.1972.160100301
17. Boyd RH (1985) Polymer 26:1123. doi:10.1016/0032-3861(85)90240-X
18. Hu WG, Schmidt-Rohr K (1999) Acta Polymerica 50:271. doi:10.1002/(SICI)1521-4044(19990801)50:8≤271::AID-APOL271≥3.0.CO;2-Y
19. Roy SK, Kyu T, St John Manley R (1988) Macromolecules 21:1741. doi:10.1021/ma00184a035
20. Ward IM, Hine PJ (2004) Polymer 45:1423. doi:10.1016/j.polymer.2003.11.050
21. Alcock B, Cabrera NO, Barkoula NM, Reynolds CT, Govaert LE, Peijs T (2007) Compos Sci Tech 67:2061. doi:10.1016/j.compscitech.2006.11.012
22. Amash A, Zugenmaier P (1997) J App Polym Sci 63:1143. doi:10.1002/(SICI)1097-4628(19970228)63:9≤1143::AID-APP6≥3.0.CO;2-H
23. Dutta NK, Edward GH (1997) J Appl Polym Sci 66:1101
24. Alcock B, Cabrera NO, Barkoula N-M, Loos J, Peijs T (2006) Composites: Part A 37:716. doi:10.1016/j.compositesa.2005.07.002